

The impact wedge-peel performance of structural adhesives

B. R. K. BLACKMAN, A. J. KINLOCH, A. C. TAYLOR, Y. WANG*

Department of Mechanical Engineering, Imperial College of Science, Technology and Medicine, Exhibition Rd., London, SW7 2BX, UK

E-mail: a.kinloch@ic.ac.uk

The impact wedge-peel (IWP) test is an International Standard (ISO 11343) method that is employed to measure the resistance to cleavage fracture of structural adhesives at a relatively high test-rate of 2 to 3 m/s. In the present work this test has been employed to evaluate the performance of a range of structural adhesives when used to bond either steel or aluminium-alloy substrates. Firstly, a novel test arrangement for performing these tests, using a high-speed servohydraulic machine, is described. Tests were performed at 10^{-4} and 2 m/s and at test temperatures of -40 and 23°C . High-speed photography was also used to investigate the failure of the IWP test specimens. Both stable and unstable types of crack growth were recorded, with the crack propagating cohesively through the adhesive layer in all cases. The methods of data analysis recommended by the International Standard are critically reviewed, and some shortcomings are highlighted. Secondly, the results from the IWP test are then directly correlated to the measured values of the adhesive fracture energies, G_c , of the adhesives, which were determined using a fracture-mechanics approach. Finally, it is demonstrated that, from knowledge of the value of G_c of the adhesive, coupled with a finite-element analysis of the IWP test geometry, the failure behaviour of the IWP specimen may be successfully modelled and predicted. © 2000 Kluwer Academic Publishers

1. Introduction

The use of structural adhesives in industry is increasing steadily, as manufacturers have become aware of the advantages that adhesives can offer, compared with conventional joining techniques, in the assembly of engineering components and structures. However, the toughness of an adhesive joint may decrease considerably under impact-loading conditions [1]. This arises because adhesives are polymeric materials that exhibit plastic and viscoelastic deformations, and thus their fracture behaviour may be very dependent upon the rate of loading and the test temperature. Hence, for applications such as in the automotive industry, for example, where adhesives are being used increasingly in safety-critical areas, it is necessary to evaluate any possible decrease in performance that may occur when the adhesively-bonded joints are subjected to impact loading. The present work discusses a test method which has recently been adopted by the automotive industry [2–5] to evaluate the fracture behaviour of adhesive joints when subjected to relatively high rates of test at various test temperatures. This is the impact wedge-peel (IWP) test, for which an International Standard (ISO 11343) test method [6] was recently adopted.

The present work firstly discusses in detail the application of this IWP test method to measure the re-

sistance to cleavage fracture of structural adhesives. In this part of the work, high-speed photography has been used to investigate the fracture behaviour of the specimen. The results from IWP tests, using a range of commercially-available structural epoxy adhesives to bond either aluminium-alloy or steel substrates, are then described. Also, the effects of changes in the specimen geometry on the impact behaviour are considered. Secondly, the IWP results are compared with the values of the adhesive fracture energies, G_c , of the various adhesives, measured using continuum fracture-mechanics methods. Finally, a finite-element model is developed to predict the value of the IWP cleavage force as the crack propagates through the specimen from the independently-measured value of the adhesive fracture energy, G_c , of the adhesive.

2. The impact wedge-peel (IWP) test

A schematic of the IWP test is shown in Fig. 1. This design is in agreement with that described in the International Standard (ISO 11343) [6]. The specimen is shaped like a tuning fork, and a wedge (of a specified shape) is drawn through the bonded portion of the specimen, as indicated in Fig. 1. The International Standard [6] specifies that specimens should be 90 mm

* Present Address: DuPont Polyester, Wilton, Middlesborough, Cleveland, TS90 8JF, UK.

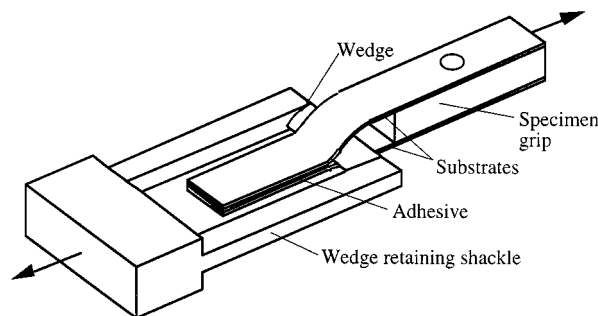


Figure 1 The impact wedge-peel (IWP) test specimen.

long and 20 mm wide, and made using sheet-metal substrates of between 0.6 and 1.7 mm thick. The substrates should be bonded over a length of 30 mm, the unbonded arms being formed to give the ‘tuning fork’ profile. No starter crack or notch is used with these specimens. The free arms of the specimen are clamped and the wedge is drawn through the bonded portion, as shown in Fig. 1. The wedge velocities recommended by the International Standard are 2 m/s for steel substrates, and 3 m/s for aluminium-alloy substrates. The methods of analysis of the test data, as recommended by the International Standard, will be discussed later.

3. Experimental procedure

3.1. Materials

A number of rubber-toughened structural epoxy adhesives were tested, and these are listed in Table I. These were chosen to represent a range of structural adhesives which possessed a wide variation in toughness. The conditions used for curing the adhesives, and the resulting glass transition temperatures, T_g , are also given in Table I.

3.2. The impact-wedge peel (IWP) test

3.2.1. Specimen preparation

The substrates used for the IWP tests were either a mild-steel substrate (Grade ‘EN3A’) or an aluminium-alloy (Grade ‘EN AW-5251’). The International Standard [6] allows the ‘tuning fork’ profile of the substrates to be formed prior to, or after, bonding. Forming the substrates prior to bonding can later result in a relatively large bead of adhesive being present in the bonded joint at the ‘V’ created by the junction where the unbonded substrate arms meet the bonded portion. Nevertheless,

work conducted by Davis and Fay [2] has shown that more consistent results may be achieved by forming the substrates prior to bonding. This observation arises because (i) forming the substrates after bonding may generate a crack in the adhesive; (ii) of the increased variability of the substrate profile produced by the more difficult process of forming profile the substrates after they have been bonded; and (iii) it may be very difficult to bend accurately relatively thick substrates by hand after bonding. Thus, in the present work, the substrates were formed prior to bonding. The excess adhesive was removed from the ‘V’ formed by the shape of the pre-formed substrates before curing the adhesives, to keep the bead size at this location to a minimum.

Therefore, the substrates were first guillotined from the metal sheet to the required size, i.e. 20 ± 0.25 mm wide by 90 ± 1 mm long. They were then preformed by clamping the portion that would be bonded later in a jig, and tapping a forming-wedge between the free arms to separate and plastically deform them, see the Appendix for details. The loading hole was drilled using the same jig, a spacer being clamped between the substrates to prevent them bending whilst being drilled.

Prior to bonding, the surfaces of the substrates were abraded by grit blasting using 180/220 mesh alumina grit, and solvent cleaned. Adhesive was then applied to each substrate, with a loop of copper wire placed in the adhesive layer to ensure a constant adhesive layer thickness of 0.4 mm. Work by Holmes [7] and Davis and Fay [2] has shown that the presence of this wire has no effect on the measured results. The substrates were brought together and clamped in individual bonding jigs, and the excess adhesive was removed prior to curing. Particular care was taken to remove as much as possible of the excess adhesive from the ‘V’ formed by the substrates before curing of the adhesive was undertaken. After curing the adhesive, any excess adhesive present around the sides of the specimen was removed with a knife, or file. Any small bead of cured adhesive remaining in the ‘V’ formed by the substrates was not removed, since its removal could lead to the formation of a crack in the specimen.

3.2.2. Testing

The tests were undertaken of the IWP specimens using a high-speed servo-hydraulic machine, as shown schematically in Fig. 2. The basis of the method is to keep the wedge stationary (via a retaining shackle) and

TABLE I Adhesives used in the current work

Adhesive	Symbol ^a	Manufacturer	Form	Cure temperature (°C)	Cure time	Glass transition T_g (°C)
‘E32’	◀	Permabond	Two-part	60	60 min	56
‘AV119’	■	Ciba Polymers	Single-part	120	60 min	113
‘ESP110’	◆	Permabond	Single-part	150	45 min	104
‘XW1044’	●	Ciba Polymers	Single-part	155	50 min	95
‘XB5315’	▲	Ciba Polymers	Single-part	190	25 min	85
‘AV4600’	▶	Ciba Polymers	Single-part	180	30 min	91
‘EA9309’	+	Hysol Dexter	Two-part	23	5 days	79
‘LMD1142’	▼	Ciba Polymers	Single-part	180	30 min	98

^aSymbols may be filled or open.

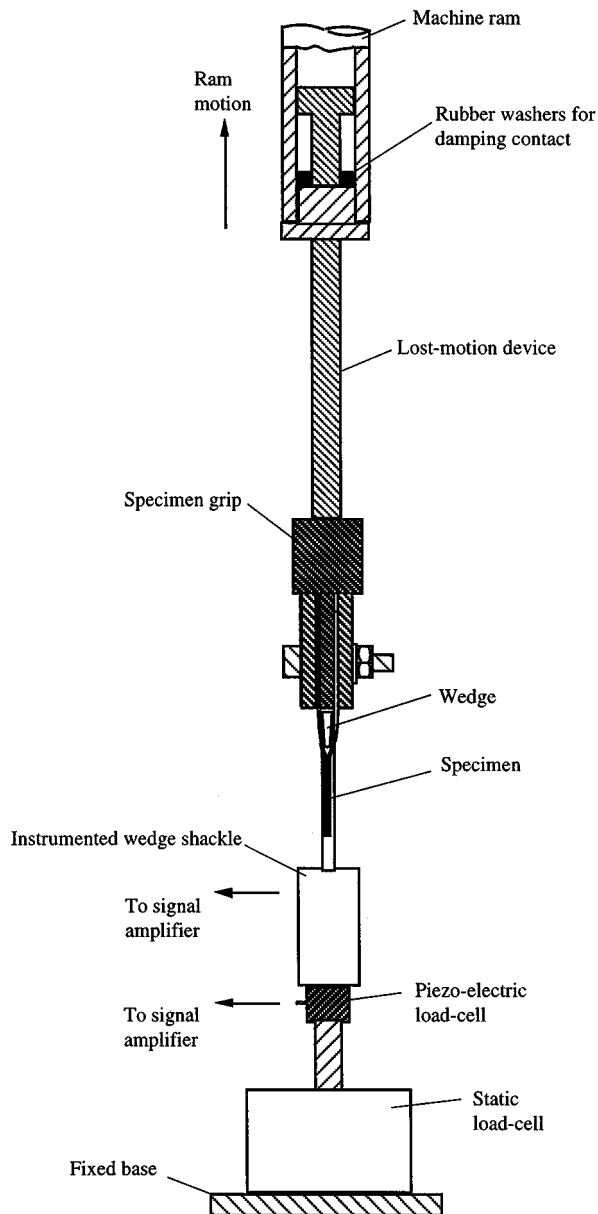


Figure 2 High-rate test apparatus for the IWP tests.

pull the specimen, which is connected to the moving ram of the test machine, through the wedge. Four repeat tests were performed for each combination of adhesive, substrate, test rate, and test temperature. For consistency and ease of comparison, the present work used a test rate of 2 m/s for both the steel and the aluminium-alloy specimens, rather than the 2 m/s and 3 m/s respectively as recommended by the Standard.

The test apparatus used a lost-motion device, which allows the ram to accelerate for a short distance so as to reach the required constant test-rate before motion is imparted to the specimen, see Fig. 2. The contact between the ram and the lost-motion device was damped using rubber washers to reduce any oscillations when the lost-motion device made contact with the ram. The specimen grip and lost-motion device were made from titanium to reduce the inertia of the system. In contrast to the recommendation of the International Standard [6], but as noted above, the IWP specimen, rather than the wedge, was attached to the moving part of the testing machine. Again, this test arrangement

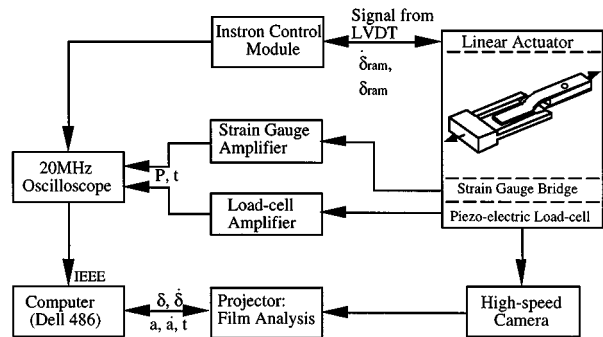


Figure 3 Schematic of testing arrangement for the IWP tests.

was designed to reduce the inertia of the system. An oscilloscope was used to record the displacement versus time output from the testing machine and the force versus time signal, as shown schematically in Fig. 3. These traces were then transferred to a computer analysis package to calculate the results. High-speed photography was also used with some tests, as described below.

A 2.5 kN piezo-electric load-cell was mounted below the wedge retaining-shackle and was initially used to measure the force, P , on the specimen, as shown in Fig. 2. However, this system was found to resonate at approximately 2 kHz. Thus, the force versus time traces produced were unsuitable for the determination of the imposed forces, due to the large oscillations superimposed on the specimen response. Therefore, strain gauges were bonded onto the arms of the wedge and connected into a bridge circuit. Analysis of the signals from individual strain gauges showed that the wedge exhibited a degree of bending in some tests. This placed the pairs of gauges into tension and compression. However, this effect cancelled out when the gauges were combined in the bridge circuit. This arrangement of strain gauges was calibrated by placing a dummy specimen in the fixtures and applying a range of constant forces. A linear variation between the voltage output of the strain-gauge bridge and the load cell force was observed. In the present work it was considered to be important not to filter any of the recorded signals, since this may lead to valuable and relevant information being lost before the test results are analysed [8, 9].

The signals from the strain-gauge bridge and the displacement, taken from a linear-variable displacement transducer (LVDT) located on the ram of the test machine, were recorded. The test (i.e. ram-displacement) rate was calculated from the gradient of the displacement versus time response. The displacement response was linear with time, and hence the test rate had a constant value of 2 m/s, as illustrated in Fig. 4.

Room-temperature tests were conducted at 2 m/s, at $23 \pm 2^\circ\text{C}$ and $50 \pm 5\%$ relative humidity, in accordance with ISO 291 [10]. In the present work, tests were also undertaken at a test rate of 10^{-4} m/s, in order to study the effect of rate. The tests at 10^{-4} m/s were conducted using the same high-speed servo-hydraulic machine, with the same test fixtures, as for the high-rate tests. The lost-motion device was still used, but the pre-travel available for acceleration was reduced from 100 mm to 10 mm.

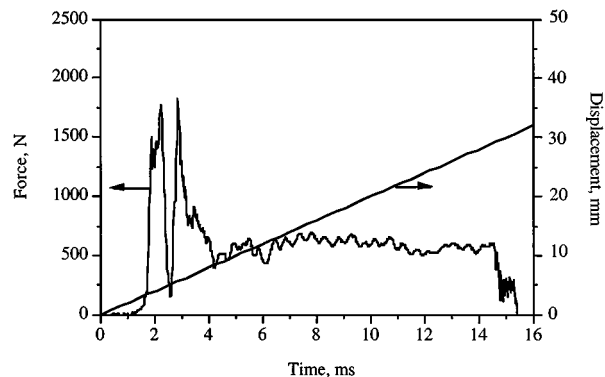


Figure 4 Force and displacement versus time response from the instrumented wedge. (Steel specimen bonded with 'XB5315' adhesive; tested at 2 m/s; stable crack growth was observed.)

Additionally, 2 m/s tests were conducted at -40°C . The -40°C tests were performed using an environmental chamber mounted on the testing machine. The time taken for the specimens to attain the test temperature was measured using a thermocouple embedded in the adhesive layer of a specimen. It was also necessary for the strain-gauge bridge to reach the test temperature, and for the output to stabilise. Thus, after the specimen was placed in the testing fixture, it was allowed to acclimatise for about fifteen minutes before being tested. The broken specimen was removed and the chamber left for a further ten minutes before the next specimen was fitted into the grips.

3.2.3. High-speed photography

To investigate the detailed failure of the IWP specimens at the relatively high test-rate of 2 m/s, a 16 mm 'Photec IV' rotating prism high-speed camera (supplied by Hadland Photonics) was used to film some of the IWP tests. The tests were filmed at a slight angle, such that the wedge retaining-shackle did not obscure the crack. The camera printed a timing mark on the film every millisecond, and these showed that a maximum framing rate of approximately 6000 pictures per second could be obtained. As a typical impact wedge-peel test at a test rate of 2 m/s lasts about 15 milliseconds, approximately ninety frames were obtained over the duration of a typical test. The specimens were illuminated with a focused tungsten spotlight. This was activated immediately before testing to prevent any heating of the specimen.

The high-speed films were projected frame by frame onto a screen, allowing measurements to be made from the greatly enlarged image. (The magnification factor of the image was calculated from the projected size of the wedge shackle for each film.) The distance from the wedge tip to the crack tip was measured from the image, as was the distance from the wedge to the end of the specimen. Thus, the crack length, a , and hence the crack velocity, \dot{a} , could be calculated. The velocity at which the specimen moved over the wedge was also calculated. It was found that for a given ram-displacement (i.e. test) rate, δ , of either 10^{-4} or 2 m/s, that the measured values of the test rate, δ , the velocity of the spec-

imen and the crack velocity through the IWP specimen when stable crack growth occurred (see below) were not significantly different.

3.3. The fracture-mechanics tests

3.3.1. Introduction

The adhesively-bonded double-cantilever beam (DCB) and tapered double-cantilever beam (TDCB) are both popular fracture-mechanics test geometries, and have been used extensively to determine the adhesive fracture energy, G_c , of bonded joints at relatively slow test rates [1, 11, 12]. An ASTM standard is available (D3433-93) [13] for slow-rate testing and recently, a new protocol has been drafted by the European Structural Integrity Society (ESIS) for these test geometries [14]. Following the increased interest in the behaviour of adhesively-bonded joints at high rates, recent work has concentrated on undertaking DCB [1, 15] and TDCB [16, 17] tests at relatively high test-rates, but at present no standards exist for such high-rate tests.

In the present work, the TDCB test has been employed to measure the adhesive fracture energy, G_c , of joints consisting of aluminium-alloy substrates bonded with each of the eight different structural epoxy adhesives listed in Table I. As described below, the rate of test has been adjusted in order to give a similar value of crack velocity as observed in the IWP tests, so that a direct correlation between the test results may be made.

3.3.2. Specimen preparation

The TDCB substrates were tapered in order to provide a linear change in compliance, C , with crack length, a . The beams were 310 mm long, 12.7 mm or 10 mm wide and the height, h , was defined by a constant, m , such that:

$$m = \frac{3a^2}{h^3} + \frac{1}{h} \quad (1)$$

with a being the crack length. For the beams employed in the current study, $m = 2 \text{ mm}^{-1}$.

Two grades of aluminium alloy, both possessing relatively high yield stresses, were used for these tests: EN AW-5083 and EN AW-2014A. The latter grade possessed the higher yield strength and it was found to be necessary to use this grade when bonding the tougher adhesives, in order to avoid plastic deformation of the substrate beams during the test. (The basis of the DCB and TDCB tests is that the substrate arms deform only in a linear-elastic manner.) Prior to bonding, the substrates were abraded by grit blasting, using 180/220 mesh alumina grit, solvent cleaned and then etched [18] in chromic acid for 30 minutes at 68°C . Adhesive was then applied to each substrate, and a double layer of aluminium foil was placed on one substrate, extending 90 mm from the loading end, such that when the joint was formed the double layer of foil would be at approximately the mid-thickness of the adhesive layer. The two layers of foil were stepped at the end, providing a foil thickness of just 13 microns at the crack tip. Wire shims of diameter 0.4 mm were inserted into the adhesive at

each end of the beam to control the thickness of the adhesive layer. All the joints were then cured according to the manufacturers' instructions, as summarised in Table I. Following curing, any excess adhesive was removed from the sides of the beam and the bonded portion was sprayed with a thin layer of white paint to assist the subsequent measurement of the crack length. Crack length markers were drawn onto each specimen. The beams used for testing at -40°C were shorter than those used for room temperature testing. This was to facilitate testing in the temperature chamber, which limited the beam length to 265 mm.

3.3.3. Testing

The experimental rig used for testing the TDCB joints was the same as that used for the IWP tests, except that different shackles were employed. The TDCB specimens were coupled to the test machine via titanium shackles with 8 mm diameter holes, which were drilled through to accept the steel loading pins. The stationary shackle was fitted to a 4.5 kN piezo-electric load cell. The operating characteristics of this load cell were: 70 kHz resonant frequency, 10 microsecond rise time and a discharge constant of ≥ 2000 seconds. The operating temperature range of the load cell was from -54 to 121°C . Tests were conducted at room temperature (i.e. 23°C) and at -40°C .

The TDCB specimens were attached to the loading shackles and simply supported at the non-loading end prior to each test. The tests at 23°C were filmed with the high-speed camera, as described previously, to record the crack length and the load-line opening displacement during the test. However, it was not possible to photograph the tests at -40°C due to the temperature chamber used which (i) prevented the illumination of the test beams, and (ii) prevented adequate line of sight for the camera.

In order to correlate values of G_c from the TDCB tests with the values of the force measured in the IWP tests at 2 m/s, the same crack velocity should be attained in both test geometries. The fracture-mechanics tests therefore had to be conducted at a test rate necessary to induce an average crack velocity of 2 m/s through the adhesive layer in the TDCB joint. Since this was the crack velocity which was recorded in the IWP tests conducted at 2 m/s, when stable crack growth was achieved, as discussed in detail below. In the TDCB test, the crack speed is a function of both the test rate, $\dot{\delta}$, and the adhesive fracture energy, G_c . Hence, the required value of $\dot{\delta}$ to induce a crack speed of 2 m/s is not known *a priori*. Therefore, the appropriate value of $\dot{\delta}$ was found experimentally by 'trial and error', and then three replicate tests were performed for each adhesive. (Some of the adhesives tested, especially at -40°C , exhibited stick-slip crack growth. In these instances the average crack velocity was calculated between the first crack initiation and the final beam failure.) The values of $\dot{\delta}$ necessary to achieve an average crack velocity of 2 m/s ranged from 0.03 m/s for the least tough adhesive, to 0.12 m/s for the toughest adhesive. The values of the average crack velocities obtained in the TDCB tests were always

within the range 2 ± 0.5 m/s. All failures were cohesive through the adhesive layer. Thus, in all the present work, the additional complication of interpreting data associated with failure along the adhesive/substrate interface does not arise.

For all the tests an oscilloscope captured the load versus time signals from the piezo-electric load-cell and these data were transferred to a computer for analysis. At the rather low test rates required for the present work, i.e. values of $\dot{\delta}$ from 0.03 m/s to 0.12 m/s to achieve the average crack velocities of 2 in the different adhesive joints, the load traces were not significantly influenced by dynamic effects. Hence, accurate values of the load could be directly deduced from the piezo-electric load-cell. Therefore, the values of G_c were, in turn, deduced directly from these measured force values. It is important to note, however, that when higher rate tests are performed, e.g. with values of $\dot{\delta}$ greater than about 1 m/s, then the dynamic effects become very significant and it is not possible to deduce accurate G_c values using the load traces. In these instances, accurate values of G_c may be deduced using the measured values of the crack length and beam opening displacement, δ , obtained from high-speed photography as reported previously [1, 16].

Finally, it should be noted that fracture-mechanics tests were also conducted to give a crack velocity of 10^{-4} m/s, as well as 2 m/s; again so that direct correlations with the corresponding IWP tests could be undertaken. To achieve a crack velocity of about 10^{-4} m/s, test rates of about 10^{-5} m/s were employed for the TDCB tests.

3.3.4. Determination of G_c values

The values of the adhesive fracture energy, G_c , have been deduced for the TDCB joint specimens using linear-elastic beam theory [19] which yields:

$$G_c = \frac{4P_c^2}{E_s B^2} \cdot m \quad (2)$$

where P_c is the load at failure, E_s is the substrate modulus, B is the width of the beam and the geometry factor, m , equals 2 mm^{-1} . The value of the modulus for the two grades of aluminium alloy used was taken to be 70 GN/m^2 . Thus, for constant values of E_s , B and m , the value of G_c depends only upon the values of the measured load, P_c , at the onset of crack growth. (When stick-slip crack propagation occurred, G_c was calculated from the load associated with crack initiation, rather than crack arrest.)

4. Analysis of the results of the impact wedge-peel (IWP) tests

4.1. Introduction

This Section discusses how the IWP test data were analysed. The method of analysis recommended by the International Standard [6] will be critically considered, and possible amendments to the method of analysis will be discussed. However, before the Standard analysis can be discussed in detail, the general failure behaviour

of the IWP needs to be considered. Thus, firstly, the types of crack growth, and the associated relationships between the measured force and time, observed for the IWP tests will be discussed. It should be noted that the loci of joint failure were always found to be via a crack propagating cohesively through the adhesive layer in the IWP joints. Thus, in all the present work the additional complication of interpreting data associated with failure along the adhesive/substrate interface does not arise.

4.2. Types of crack growth

4.2.1. Introduction

The crack was found to propagate through the adhesive layer by one of either two types of growth: (i) via a stable form of crack growth, or (ii) via an unstable form of crack growth. An example of the force versus time trace of an IWP test which exhibits stable crack growth is shown in Fig. 4, whilst Fig. 5 compares the typical traces for both stable and unstable crack growth.

4.2.2. Stable crack growth

A typical IWP force versus time trace, when stable crack growth occurs, consists of one or two initial peaks followed by a 'plateau' region where the measured force is approximately independent of the time axis, as shown in Fig. 4. From the high-speed photography studies, the initial peak occurs when the wedge first makes contact with the specimen, and a crack then initiates and propagates through the specimen. However, this initial crack runs for only about 5 mm and then arrests. This short burst of unstable crack growth gives rise to the first peak. Frequently, this process is repeated, which gives rise to a second peak in the force versus time trace. These initial peaks arise from dynamic effects, as the wedge first makes contact with the specimen, and from the formation of a sharp crack from the blunt edge, or bead, of the adhesive which was formed in the 'V' of the specimen, as discussed above. This sharp crack which is generated then propagates in

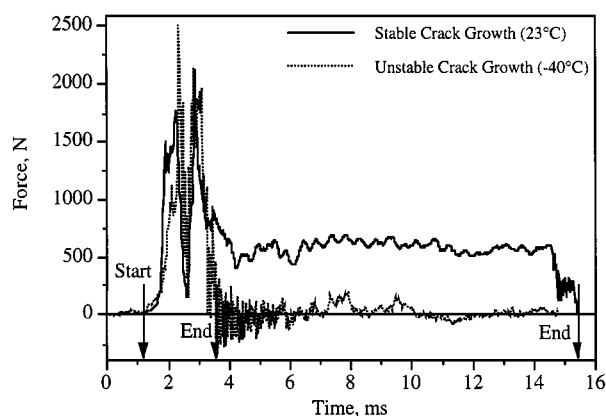


Figure 5 Force versus time responses from impact wedge-peel specimens showing stable and unstable crack growth. The 'start' and 'end' points of the crack propagating through the specimen, discerned using high-speed photography, are marked on the traces. (Steel specimens bonded with 'XB5315' adhesive; tested at 2 m/s and at 23 and -40°C . Failed specimens are shown in Fig. 6.)

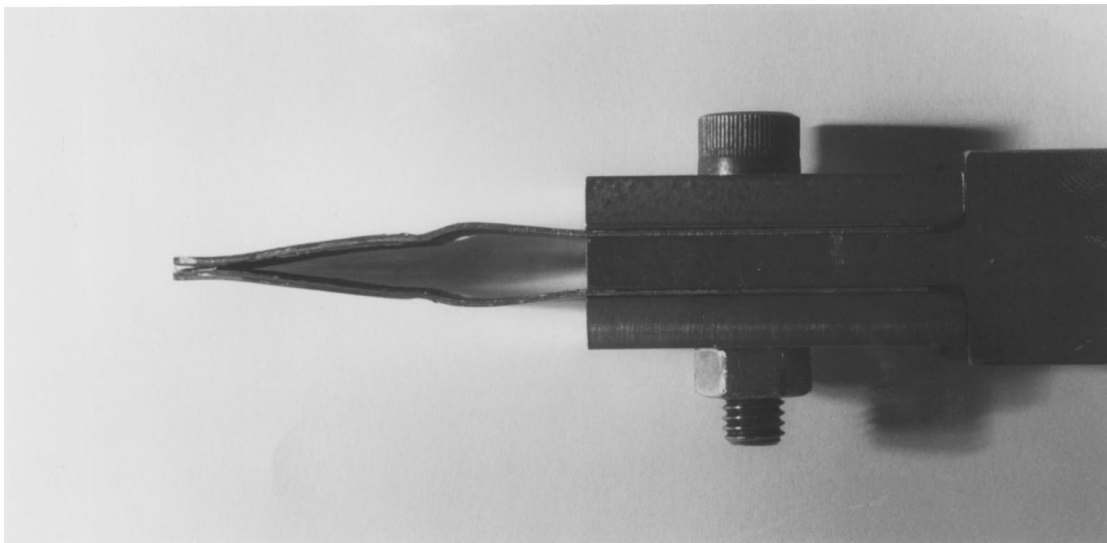
a stable manner through the specimen, giving rise to the 'plateau' region which is observed.

This stable 'plateau' region typically lasts for approximately 10 ms for a test undertaken at 2 m/s. Analysis of the high-speed films shows that the crack velocity is equal to the test rate over this region, and there is typically about 20 mm of stable crack growth in the 'plateau' region for the IWP tests conducted in the present work. Indeed, for such stable crack growth, at both the test rates used, i.e. 10^{-4} and 2 m/s, the crack velocity is virtually constant throughout the 'plateau' region shown in Fig. 4, and is equivalent to the test rate. Observations of tests conducted at 10^{-4} m/s revealed that the crack tip is a constant distance ahead of the wedge over this portion of the test. Further, the smaller this distance, the higher the recorded 'plateau' force. Analysis of the high-speed films confirmed that this was also the case for tests undertaken at a rate of 2 m/s.

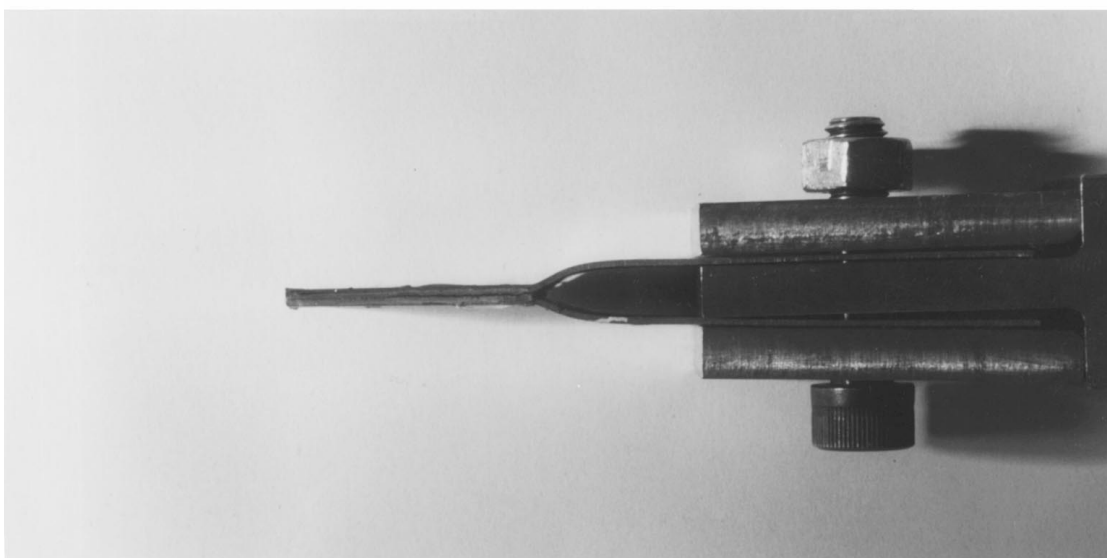
Towards the end of the test, the distance from the crack tip to the wedge increases, causing a decrease in the recorded force. This was observed both visually at a test rate of 10^{-4} m/s, and by analysis of the high-speed films of the 2 m/s tests. This effect can be seen in Fig. 4, after an elapsed time of about 14.5 ms, and is probably caused by changes in the compliance of the specimen as the crack tip approaches the end of the specimen.

Specimens that exhibit a stable 'plateau' region in their force versus time trace, as shown in Fig. 4, also tend to exhibit considerable plastic deformation of the substrates, see Fig. 6a. Indeed, it was noted from the calculated results (see below), and by direct observation of the degree of plastic deformation of the substrates after joint failure, that a relatively large amount of energy is absorbed during stable crack growth, especially in comparison with the specimens that exhibited no stable crack growth. Further, as might be expected, for those joints that exhibited stable crack growth, there was a general correlation between the measured impact resistance of the joints and the degree of plastic deformation of the substrates that accompanied failure of the joint.

Many of the above points may also be clearly seen in the sequence of high-speed photographs shown in Fig. 7 for a specimen which exhibited stable crack growth. These photographs are for an IWP test of an aluminium-alloy joint bonded using 'LMD1142' at a test rate of 2 m/s. The camera was placed at a slight angle to the plane of the specimen, so that the full width of the specimen was viewed. In Fig. 7, the tuning-fork shaped IWP specimen is being pulled through the wedge, by the arms of the specimen being pulled from the right-hand side of the photographs. The reflective wedge can be seen as the white object in about the centre of the photographs, and the numbers '2' and '4' are painted on the near-hand and far-hand sides of the wedge support arms, respectively. From Fig. 7, it may be seen that the crack tip is an approximately constant distance ahead of the wedge until complete failure of the specimen. For these IWP joints, this distance is about 6 mm. Also, the relatively large degree of plastic deformation of the aluminium-alloy arms of the specimen is clearly visible. This observation is in agreement with the above



(a)



(b)

Figure 6 Failed impact wedge-peel specimens showing the extent of plastic deformation of the substrate arms, (steel specimens bonded with 'XB5315' adhesive; tested at 2 m/s). (a) stable crack growth showing extensive plastic deformation of substrates, tested at 23°C, (b) unstable crack growth showing little plastic deformation of substrates, tested at -40°C. (Specimens are clamped in the specimen grip.)

interpretation of the force versus time curve: the plastic deformation occurs early on in the test and is associated with the presence of a stable 'plateau' region in the measured force trace.

4.2.3. Unstable crack growth

Specimens which exhibit unstable crack growth typically show a force versus time response similar to that shown in Fig. 5 for a test conducted at 2 m/s and at -40°C. The response in the initial region of the force versus time trace is similar to that seen when stable crack growth develops, namely the crack initiates, and may then arrest and initiate again. This again gives rise to one or two initial peaks. However, the crack does not now settle into a period of stable crack growth, as described above. Instead, the crack propagates very rapidly, and completely, through the specimen.

From previous work [20, 21], it is suggested that the reason for the unstable crack growth is that the wedge impacting the specimen initially gives rise to a relatively blunt crack, or notch, when it first makes contact with the adhesive bead formed in the 'V' of the specimen. However, in the case of the more brittle adhesives, the blunt crack rapidly sharpens to form a 'naturally-sharp' running crack. Thus, soon after the onset of crack growth, the rate of release of energy will be greater than that required for a stable crack, so the crack will rapidly accelerate. Hence, unstable crack growth results. Indeed, for example, a crack velocity of 30 m/s was measured, via high-speed photography, for the unstable failure of the IWP specimen tested at 2 m/s and referred to in Fig. 5. Such high crack velocities result in a very short time to failure, of the order of 1 to 2 ms, compared with about 15 ms when stable crack growth is observed.

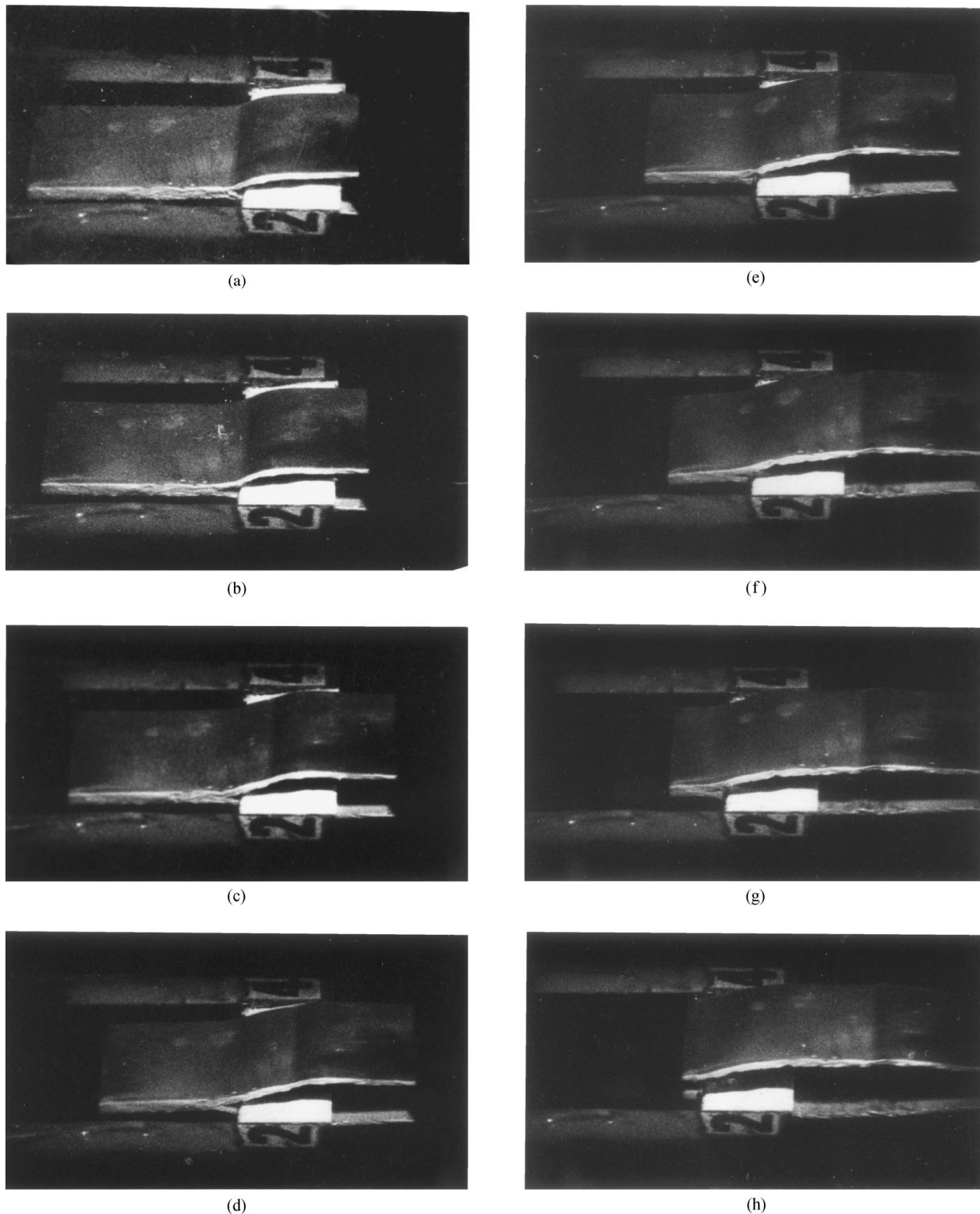


Figure 7 High-speed photographic sequence of an IWP test at 2 m/s. The adhesive was 'LMD1142', the substrates were aluminium alloy, and the camera was operated at 2000 frames per second with 16 mm Ilford FP4 black and white film. Frames indicate an elapsed time (in milliseconds) of: (a) 0 ms, (b) 2 ms, (c) 4 ms, (d) 6 ms, (e) 8 ms, (f) 10 ms, (g) 12 ms and (h) 14.5 ms (complete failure of the specimen). (The IWP specimens were 20 mm in width.)

Also, as would be expected, very little energy is absorbed by the specimen during unstable failure, and this is reflected by very little plastic deformation of the substrates being observed, as may be seen from Fig. 6b. (As well as from the calculated energy values which are discussed later.) Indeed, a visual comparison of the failed test specimens revealed that the specimen that exhibited unstable crack growth only tended to undergo

plastic deformation of the substrate arms outside of the bonded area of the joint, i.e. where the wedge first made contact with the unbonded substrate-arms and tended to straighten somewhat the substrate arms. This represents a comparatively limited degree of plastic deformation compared with that seen in the specimen that exhibited stable crack growth, where significant plastic deformation of the once-bonded area of the substrate arms also

occurred. Again, this is evident from the photographs shown in Fig. 6.

4.3. Data analysis

4.3.1. Stable crack growth

The ISO Standard specifies that the average cleavage force is calculated from the force versus time trace of the IWP test specimen, but disregarding the first 25% and the last 10% of the curve. (This is illustrated in Fig. 8 for a test where stable crack growth occurred.) The associated energy absorbed during the IWP test is calculated by integrating over the same portion of the force versus time curve, and then multiplying by the test rate. However, to be able to define the first 25% and last 10% of the curve, the ‘start’ and ‘end’ of the curve need to be defined. As the ISO Standard does not define these points, the following definitions are suggested for the IWP tests where stable crack growth is observed. The start of the curve is taken as the time at which the tensile force consistently first deviates from zero. The end of the curve is the time at which the first zero or compressive value of the force is recorded after the ‘plateau’. It should be noted these definitions agree with the start and end of the tests as observed using high-speed photography, which are marked by the onset of crack growth and the complete failure of the specimen.

These definitions have been used for the force versus time trace of the IWP test which is shown in Fig. 8. The resulting average cleavage force and energy values are quoted in Table II. However, it should be emphasised that the trace shown in Fig. 8 is associated with stable crack growth, i.e. it displays initial peaks but these are followed by a ‘plateau’ region, where stable

TABLE II Impact wedge-cleavage force and energy values calculated by the ISO Standard method for steel specimens bonded with ‘XB5315’ adhesive tested at 2 m/s. (Data from a single test at each temperature, force versus time responses shown in Figs 8 and 9.)

Test temperature (°C)	Type of crack growth	ISO Standard method	
		Cleavage-force (N)	Energy (J)
23	Stable	570	9.8
−40	Unstable	1170	3.5

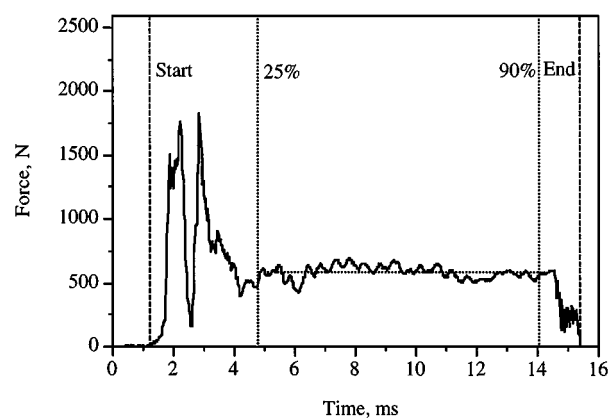


Figure 8 Impact wedge-peel test, which exhibited stable crack growth, showing the ISO Standard method of data analysis. (Steel specimen bonded with ‘XB5315’ adhesive; tested at 2 m/s and 23°C.)

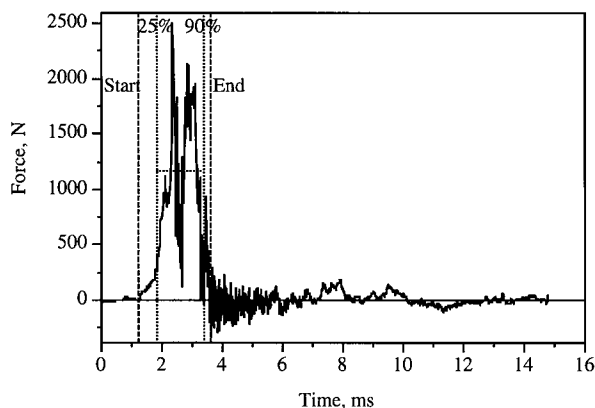


Figure 9 Impact wedge-peel test, which exhibited unstable crack growth, showing the ISO Standard method of data analysis. (Steel specimen bonded with ‘XB5315’ adhesive; tested at 2 m/s and −40°C. Compare with Fig. 8.)

crack growth occurs, as discussed above. For such a stable crack growth test the ISO Standard method of data analysis may indeed be readily used, employing the relevant definitions given above, to calculate with confidence the average wedge-cleavage force and energy values from within the ‘plateau’ region.

4.3.2. Unstable crack growth

However, as noted above, some IWP tests do not show this stable ‘plateau’ region, but fail in an unstable manner, as illustrated in Fig. 9. Furthermore, the end point of such unstable tests may not be self-evident from the force versus time response, although it may be obtained from high-speed photography. Unfortunately, if we now simply apply the ISO Standard method of data analysis to specimens which fail in such an unstable manner, then the initial peaks (associated with the dynamic effects and the initiation of a sharp crack) are incorrectly included in the results. This may be seen from Fig. 9. Thus, when unstable crack growth occurs, the ISO Standard analysis method calculates a large cleavage force, indicative of a ‘tough’ adhesive, although the joint is actually exhibiting unstable, brittle behaviour. Indeed, the ISO Standard analysis method for the unstable test at −40°C gives a value for the average cleavage force which is far greater in value than that for the stable specimen tested at 23°C, see Table II. Therefore, the values of the wedge-cleavage force calculated using the basic ISO Standard method apparently indicate that the specimen which exhibits unstable failure at a low test temperature is tougher than the specimen which exhibited stable failure at a higher temperature. From examining Figs 6, 8 and 9, and from examining the values of the associated energy absorption (see Table II), this is obviously not an accurate reflection of the relative performance of the two IWP specimens. Thus, the basic method of analysing the IWP test results proposed by the ISO Standard fails to give an accurate measure of the impact behaviour of the IWP specimen when unstable crack growth occurs.

As may be seen from Fig. 9, the ISO Standard method of analysis will probably always produce misleading results when analysing force versus time traces which

are associated with unstable failure. The Standard does state that “if the material being tested provides force curves which are highly irregular, then the test result should be discarded”. However, what constitutes a ‘regular’ or an ‘irregular’ trace is not defined in the Standard. One answer to this dilemma is, of course, to interpret ‘highly irregular’ to mean unstable failure—but if an operator has only tested adhesives that exhibit unstable failure, then these will actually all appear to be ‘regular’.

Now, several different schemes have been considered to overcome these various problems [21]. The following scheme is proposed as the best available option, and has been used in the present work. Unstable failure is said to occur when there is no ‘plateau’ region observed in the associated force versus time trace, or when the time to failure is less than 7 ms. In these cases, a zero force value should simply be quoted. Thus, in direct contrast, stable failure occurs when there is a ‘plateau’ region observed in the associated force versus time trace and when the time to failure is more than 7 ms, and in such circumstances the values of force associated with the ‘plateau’ region may be analysed and quoted.

Thus, this proposed approach overcomes the problem that the Standard method indicates ‘excellent’ joint performance when unstable failure occurs and the force versus time curve is most likely to be dominated by dynamic and associated effects. That is, when the joint performance is, in fact, probably relatively poor, and accurate values of the force for crack growth through the IWP test specimen cannot be ascertained.

4.4. Effect of specimen geometry

The ISO Standard does not specify what profiles are to be used for the IWP specimens. Clearly, the shape of the profile may affect the force versus time trace measured for the IWP test, since the shape of the substrates will influence the extent of plastic deformation of the substrates which accompanies failure of the specimen. To explore this aspect of the test, two different profiles, both within the specification of the ISO Standard, were investigated, as shown in Fig. 10. For these studies an adhesive, and a test temperature, were selected so as to give stable crack growth, with an associated ‘plateau’ region present in the force versus time trace.

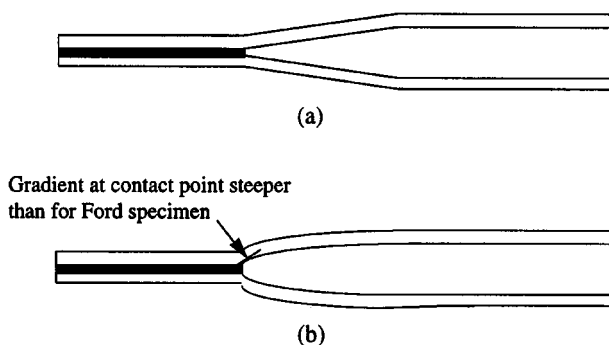


Figure 10 IWP specimen designs used by Ford and by Imperial College, showing differences in geometry at the wedge contact point. (a) Ford specimen design, shallow taper, (b) Imperial College specimen design, steep taper.

The two different IWP specimen geometries are shown schematically in Fig. 10. One design of IWP test specimen, used by workers [2] at the Ford Motor Co., tapers at a relatively shallow angle from the open end to the adhesive layer, compared with the Imperial College design used in the present work. (The latter design actually follows more closely the steep profile drawn in the ISO Standard, although both designs are within the specification of the ISO Standard.) The differences in the profile arise from the manufacturing process used to preform the substrates. The substrates for the Ford specimens are pressed individually, whilst the Imperial College design uses a forming wedge and jig to preform a pair of substrates, as described in the Appendix.

A result of the slightly different designs is that the Imperial College design of IWP specimens possess a higher effective stiffness, so the initial gradient of the force versus time response is steeper, as shown in Fig. 11. Thus, less energy is absorbed in the initial portion of the force versus time response, i.e. the portion which is associated with dynamic effects and that occurs before the ‘plateau’ region. The extent of the initial unstable crack propagation associated with these dynamic effects in a specimen with a steep profile is also greater. Thus, the remaining length of the IWP specimen is shorter when the transition to stable crack growth does occur. Hence, the ‘plateau’ region is less extensive and less energy is absorbed in this portion of the test, as shown in Fig. 11 and the results quoted in Table III.

TABLE III Impact wedge-peel force and energy values for the Ford and Imperial College specimens. (Steel specimens bonded with ‘XB5315’ adhesive; test temperature 23°C and rate of 2 m/s, force versus time responses shown in Fig. 11.)

Specimen type	ISO Standard method ^a	
	Cleavage force (N)	Energy (J)
Ford	585 ± 40	11.9 ± 0.6
Imperial College	553 ± 25	8.9 ± 0.9

^aStandard deviations shown.

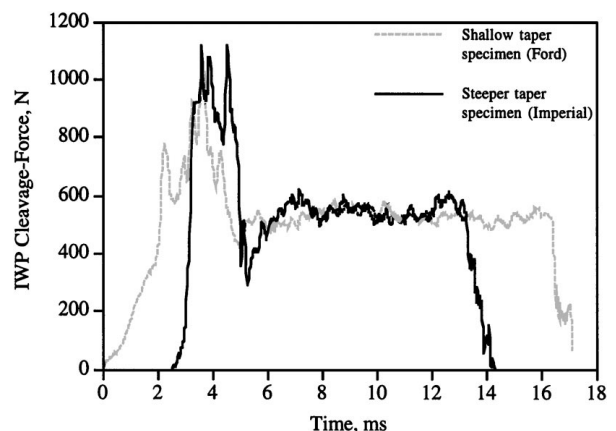


Figure 11 Force versus time responses of IWP specimens using Ford and Imperial College specimen designs. Specimen designs are shown in Fig. 10. (Steel specimens bonded with ‘XB5315’ adhesive; tested at 2 m/s and 23°C. Note that the trace from the Imperial College specimen has been slightly displaced to the right for ease of comparison.)

TABLE IV Values of G_c obtained from the TDCB tests for the eight adhesives, at various crack velocities and test temperatures

Adhesive	Symbol ^d	G_c (kJ/m ²) [Average \pm SD]		
		10 ⁻⁴ m/s, 23°C	2 m/s, 23°C	2 m/s, -40°C
'E32'	◀	0.65 \pm 0.06	0.56 \pm 0.07	0.23 \pm 0.01
'AV119'	■	0.70 \pm 0.07	0.66 \pm 0.03	0.32 \pm 0.08
'ESP110'	◆	1.06 \pm 0.02	0.81 \pm 0.02	0.38 \pm 0.02
'XW1044'	●	1.05 \pm 0.07	1.17 \pm 0.04	1.02 \pm 0.08
'XB5315'	▲	1.55 \pm 0.12	1.44 \pm 0.14	0.93 \pm 0.07
'AV4600'	▶	n/d	n/d	1.14 \pm 0.15
'EA9309'	+	3.76 \pm 0.09	3.36 \pm 0.32	n/d
'LMD1142'	▼	4.59 \pm 0.05	4.25 \pm 0.08	n/d

^an/d: not determined.

^bLocus of failure always cohesive through the adhesive layer.

^cStandard deviations are shown.

^dSymbols may be filled or open.

The importance of the above effects is that, firstly, the average cleavage force calculated using the ISO Standard method from the data shown in Fig. 11 is the same for both designs of specimen. Secondly, however, the calculated energies differ considerably, as revealed by the results given in Table III. Thus, when comparing the results from IWP specimens with different profiles, it is not possible to quote an absolute value of the energy absorbed, since the values calculated by the Standard method may differ considerably from one specimen design to another. Hence, in the present work, only the average cleavage forces of the 'plateau' region, as defined in Fig. 8, are quoted.

5. Values of the adhesive fracture energy, G_c

Values of the adhesive fracture energy, G_c , determined using the TDCB adhesive joint specimens, are given in Table IV. The main use of these data in the present work is to provide a basis for understanding and modelling the IWP results. However, some other noteworthy points do emerge from the results shown in Table IV.

Firstly, comparing the various structural adhesives employed, then a wide range of values of G_c were indeed achieved. This was one of the aims of this part of the study. Secondly, the values of G_c determined at 23°C at the two different crack velocities of 10⁻⁴ and 2 m/s clearly demonstrate that over this range of test rates the values of G_c are not greatly dependent upon the test rates employed. Although a decrease in the value of G_c is generally seen as the crack velocity is increased. Thirdly, the effect of decreasing the test temperature is to decrease the value of G_c , as would be expected.

6. Correlations between IWP results and values of G_c

6.1. Introduction

As discussed above, IWP tests were conducted at 2 m/s at room temperature (i.e. 23°C), as recommended by the ISO Standard. Additional tests were also performed at -40°C, since this temperature is considered to be the lowest likely service-temperature to be experienced by these adhesives in automotive applications. For these low-temperature tests, a rate of 2 m/s was again employed. Also, to increase the test data available for comparison with the fracture-mechanics results (given

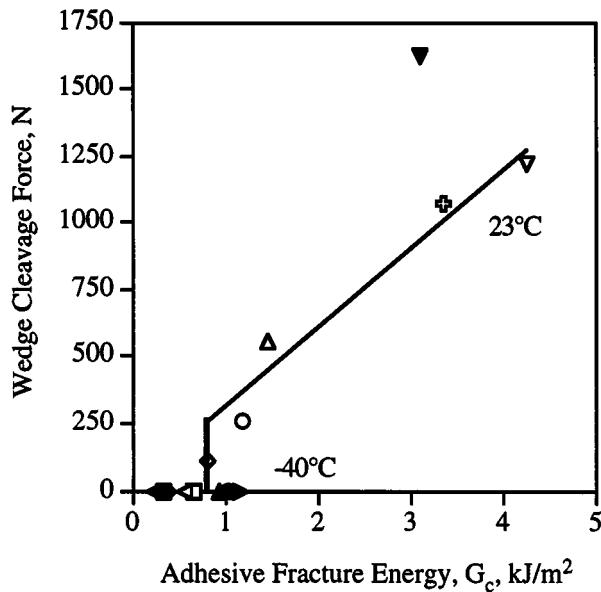
in Table IV), and to study the effect of test rate, IWP tests were conducted at the relatively slow test rate of 10⁻⁴ m/s, at 23°C. As discussed above in detail, if stable failure occurred then all the IWP test data were analysed by calculating the average 'plateau' force between 25% and 90% of the total time-to-failure. If unstable failure occurred, a zero value of the wedge-cleavage force was quoted. Also, it should be recalled that the locus of failure for both the IWP and the TDCB specimens was always cohesive in the adhesive layer. This obviously greatly facilitates any attempt to achieve a direct correlation between the two different types of test. Finally, it should also be recalled that the tests on the IWP and the TDCB tests were undertaken to give similar values of the crack velocities in the two different types of test; i.e. either approximately 2 m/s or 10⁻⁴ m/s.

An initial comparison between the values of the adhesive fracture energy, G_c , (see Table IV) and the corresponding energies dissipated during typical IWP tests where stable crack growth was observed (see Table II) reveals that the values of G_c are far lower than the energies per unit area associated with the IWP tests. For example, for the 'XB5315' adhesive the value of G_c is 1.44 kJ/m² at 23°C whilst the IWP test energy, using steel substrates, is about 16 kJ/m². Clearly, much of the excess energy has been used in plastic deformation of the substrate arms, see Fig. 6a. (However, for the reasons stated previously, the following correlations are undertaken using values of the IWP cleavage force, rather than the measured energies.)

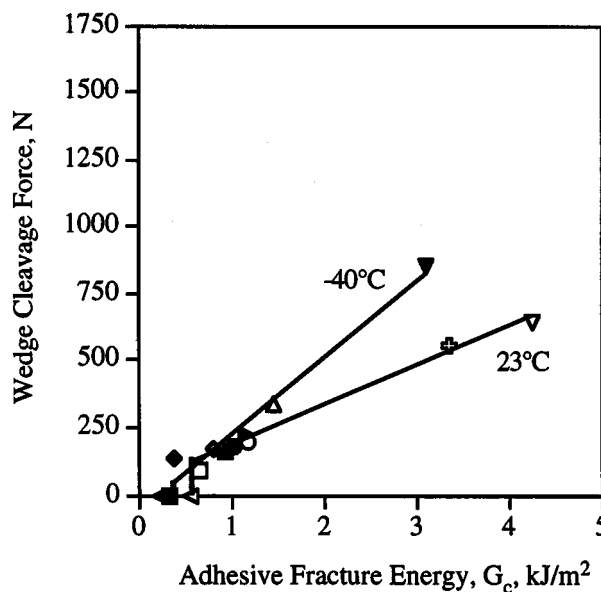
6.2. Effect of test temperature and substrate type

IWP tests were performed at -40 and 23°C, at a test rate of 2 m/s, for both steel and aluminium-alloy substrates. The values of the adhesive fracture energies, G_c , were also measured using the TDCB specimens at the relevant test temperature and at a crack velocity of 2 m/s, which was equivalent to the crack velocity during the IWP tests which exhibited stable crack growth.

The results for both the steel and aluminium-alloy IWP tests, shown in Fig. 12a and b, respectively, reveal linear correlations between the measured IWP cleavage force and the corresponding value of the adhesive fracture energy, G_c . However, the relationships between



(a)



(b)

Figure 12 IWP cleavage force versus adhesive fracture energy, G_c , at -40°C (filled points) and 23°C (open points). (a) steel substrates, (b) aluminium-alloy substrates. (Crack velocities were 2 m/s. See Table I for identification of adhesives.)

the IWP cleavage force and the adhesive fracture energy do not pass through the origin. Instead, there is a lower-limit to the value of G_c , below which the corresponding IWP cleavage force is zero, due to unstable crack growth occurring in the IWP test. Indeed, the presence of such a limiting value of G_c was also confirmed by other observations made during the course of these studies, as discussed below.

In the case of the IWP specimens made using the steel substrates and tested at 23°C (see Fig. 12a), this lower-limit of the value of G_c is approximately equal to the adhesive fracture energy of the 'AV119' adhesive. Since, it was observed that several of the 'AV119'/steel IWP specimens failed via unstable crack growth, whilst the remainder failed in a stable manner. This gives a value of the limiting adhesive fracture energy of about

0.66 kJ/m^2 , for these test conditions and for the IWP steel specimens. Thus, as would be predicted from these arguments, since the more brittle 'E32' adhesive has a lower value of G_c of 0.56 kJ/m^2 , then all of the IWP tests prepared using this adhesive failed in an unstable manner and, hence, with a recorded IWP cleavage force of zero.

In the case of the steel IWP specimens tested at -40°C , unstable crack propagation was always observed, except for the toughest adhesive (i.e. the 'LMD1142' adhesive). Thus, apart from the IWP steel/'LMD1142' tests, zero values of the wedge cleavage forces were always recorded. Hence, from Fig. 12a, it may be seen that the limiting value of the adhesive fracture energy, G_c , in the case of the IWP steel substrates is significantly higher at -40°C , compared to 23°C . Indeed, it must be greater than about 1.14 kJ/m^2 at -40°C , compared with about 0.66 kJ/m^2 at 23°C . This effect is probably due to an increase in the yield stress, σ_y , of the steel substrates at the lower test temperature. The value of σ_y increases by about 10% as the temperature is reduced from 23°C to -40°C , whilst the modulus of the steel substrates is unaffected by this temperature change [22, 23]. Now, this increased yield stress will result in a larger applied force being required to plastically deform the steel substrates and, hence, a tougher adhesive is required to enable these higher required stresses for plastic deformation of the steel arms to be attained during the IWP test. Thus, a higher value of the limiting value of G_c is observed at the test temperature of -40°C .

Fig. 12b shows the relationship between the IWP cleavage force and the corresponding value of the adhesive fracture energy, G_c , for the IWP tests using aluminium-alloy substrates. Similar effects may be observed to those described above for the steel IWP tests, except that the limiting value of G_c appears to be not so greatly affected as the temperature is decreased. This may be explained by the modulus and yield stress of aluminium alloy not being so significantly affected by the change in test temperature [24, 25].

Fig. 13 shows a comparison between the results for the steel and aluminium-alloy IWP tests at a test temperature of 23°C , and at a crack velocity of 2 m/s. For a given adhesive, then when stable crack growth occurs, different values of the IWP cleavage force are recorded, depending upon whether steel or aluminium-alloy substrates were used to prepare the IWP test specimen. It should be noted that higher forces were recorded for the steel substrates, especially for the tougher adhesives. This effect may be explained by the higher stiffness and yield stress of the steel arms, compared with the aluminium-alloy substrate arms, which means that a larger cleavage force is required to separate and plastically deform the steel substrates to enable the wedge to pass between them. (The yield stresses of the steel and aluminium-alloy substrates were measured to be 180 MN/m^2 and 140 MN/m^2 respectively [21], see Table V.) Also, the limiting value of G_c for the adhesive for the steel IWP joints appears to be somewhat higher than that recorded for the aluminium-alloy joints. From the above arguments, the higher yield stress for the steel

TABLE V Material properties used for finite-element modelling. (Terms are defined in Fig. 15. Modulus and yield data for substrate materials are from tensile tests. Epoxy adhesive data are taken from the literature [26])

Property		Steel 'EN 3A'	Aluminium alloy 'EN AW-5251'	Epoxy adhesive
Modulus	E (GN/m ²)	206	69	3.0
Yield stress	σ_y (MN/m ²)	180	140	—
Fitting stress	σ_p (MN/m ²)	250	160	—
Plastic strain	ε_p (%)	1.1	0.6	—
Poisson's ratio	ν	0.33	0.33	0.4

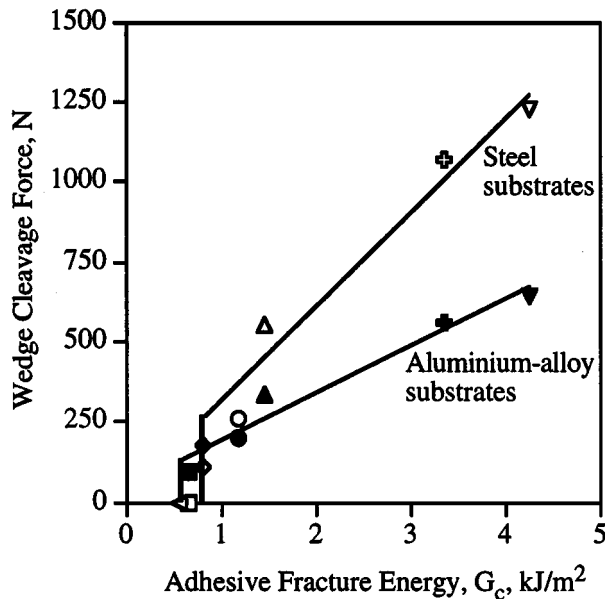
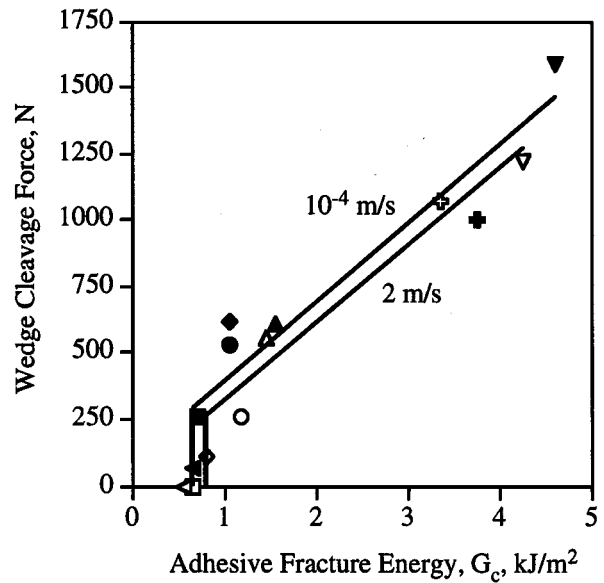


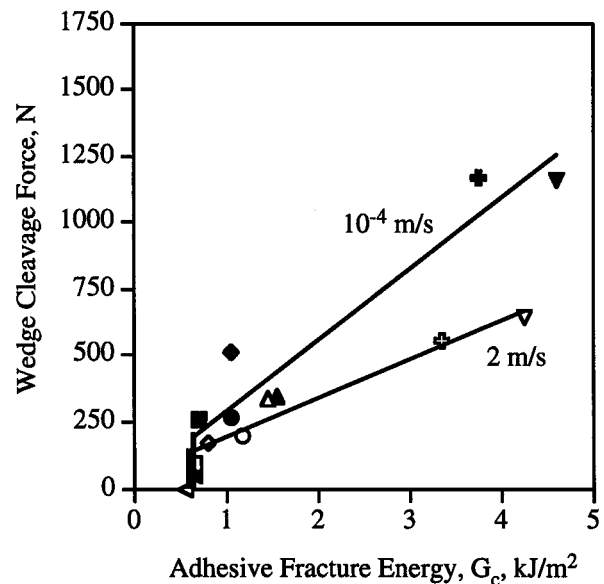
Figure 13 IWP cleavage force versus adhesive fracture energy, G_c , at 23°C and at a crack velocity of 2 m/s. Steel substrates (open points) and aluminium-alloy substrates (filled points) used for the IWP test. (See Table I for identification of adhesives.)

substrates would indeed be expected to be associated with an increase in the limiting value of G_c for the adhesive in the case of the IWP steel joints. Thus, the relatively higher modulus and yield stress of the steel arms, compared to the aluminium-alloy arms, lead to an increase in the limiting value of G_c , above which stable crack growth is observed to occur. Furthermore, once stable crack growth does occur, and the substrate arms now undergo significant plastic deformation, the cleavage force associated with this process will be higher for the steel, as opposed to the aluminium-alloy, arms.

Therefore, to summarise, when the measured IWP cleavage forces are plotted against the corresponding value of the adhesive fracture energies, G_c , then a noteworthy point is that there is a limiting value of G_c . Below this limiting value, the toughness of the adhesive is inadequate to enable sufficiently high stresses to be developed in the substrates to give rise to extensive plastic deformation of the substrates. Hence, below this limiting value of G_c , unstable crack growth is seen in the IWP test specimen and a zero value of the wedge cleavage force is recorded. It should be noted that the value of this limiting G_c parameter must clearly be dependent upon the elastic-plastic response of the substrate, as was indeed observed.



(a)



(b)

Figure 14 IWP cleavage force versus adhesive fracture energy, G_c , at crack velocities of 10^{-4} m/s (filled points) and 2 m/s (open points) at 23°C. (a) steel substrates, (b) aluminium-alloy substrates. (See Table I for identification of adhesives.)

6.3. Effect of crack velocity

The effect of crack velocity is shown in Fig. 14 and, as before, these data have been plotted in the form of the values of the IWP cleavage forces versus the corresponding values of the adhesive fracture energies, G_c . As may be seen from Fig. 14, for both the steel and the aluminium-alloy substrates, the measured IWP cleavage forces are somewhat greater for the lower crack velocity of 10^{-4} m/s, than for the 2 m/s tests. This reflects the trends seen for the values of G_c , as discussed above and shown in Table IV. Thus, the relationship between the cleavage force and G_c is also dependent upon the crack velocity attained in the test. However, the relationship between the wedge cleavage force and G_c is still essentially linear, as shown in Fig. 14.

At both crack velocities, the gradient of the linear relationship between the IWP cleavage force and adhesive

fracture energy is steeper when steel substrates, as opposed to aluminium-alloy substrates, are used for the IWP specimens. As commented above, this difference may be explained by the higher stiffness and yield stress of the steel arms compared to the aluminium-alloy substrate arms. This leads to a larger cleavage force being required to separate and plastically deform the arms of the steel substrates in order to enable the wedge to pass between them—which will occur providing the value of G_c of the adhesive employed is above the limiting value and hence will allow such relatively high stresses to be attained in the arms of the substrate without premature, unstable, cracking of the adhesive intervening.

7. Modelling studies

7.1. The finite-element model

A finite-element (FE) model of the impact wedge-peel test was developed using the 'ABAQUS' commercial FE package. The unbonded region of the specimen and the 30 mm bonded length of the IWP specimen were modelled. In the two-dimensional model used the adhesives and substrates were modelled using eight-noded quadratic elements. Due to symmetry it was only necessary to model half of the specimen, and plane-strain conditions were assumed for all cases. The mesh used consisted of 1400 elements, and is shown in Fig. 15. Contact elements were used along the fractured sur-

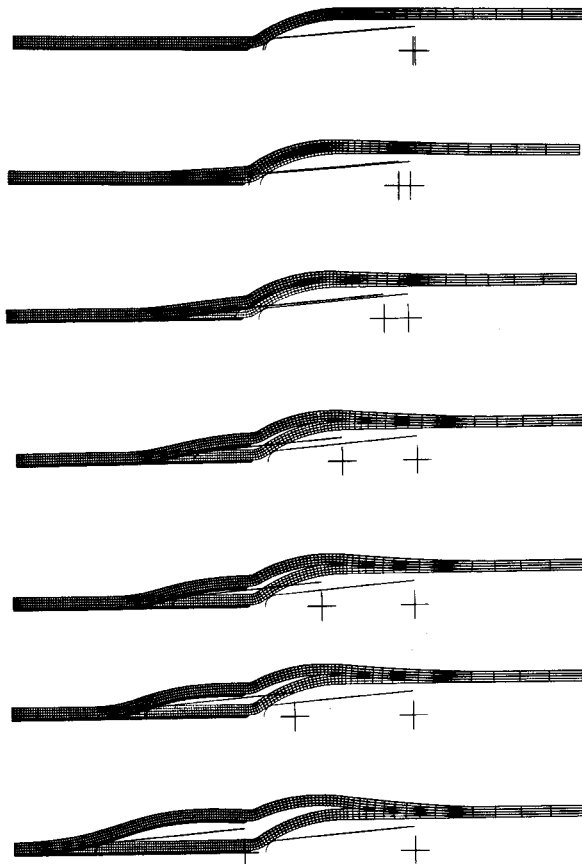


Figure 15 Series of finite-element predictions, from initial contact to final failure, of an aluminium-alloy impact wedge-peel specimen bonded with the 'XB5315' adhesive being tested at 10^{-4} m/s. The initial, undeformed, mesh is shown together with the displaced mesh. The elapsed times are 1, 6, 15, 35, 45, 60 and 85 s respectively, from top to bottom. The '+' symbol indicates a reference point on the wedge.

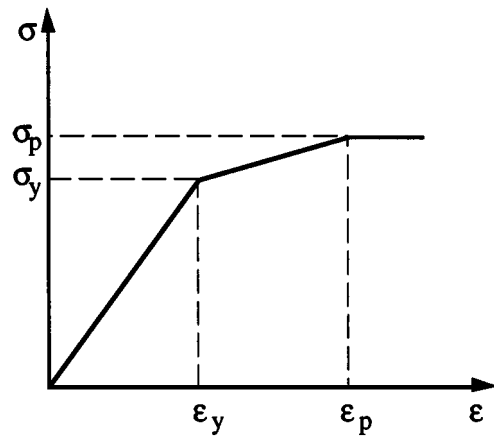


Figure 16 General material model used in finite-element model.

face of the adhesive and along the unbonded surface of the substrates. Contact between the wedge and the surface was assumed to be rigid-elastic in nature. The effects of friction between the wedge contact point and the substrate or fractured surface of the adhesive were also modelled, as discussed later.

The steel and aluminium-alloy substrates were modelled as bilinear work-hardening materials, as shown schematically in Fig. 16. Uniaxial tensile tests were performed using the substrate materials at a test rate of 10^{-4} m/s, to provide the modulus and yield data, see Table V. The adhesive was assumed to be a bulk linear-elastic material, using published data [26] which are also given in Table V. Insufficient high-rate data concerning the basic properties of the adhesives and substrates were available, so all the modelling studies were based upon an IWP test rate of 10^{-4} m/s, and undertaken at a test temperature of 23°C . A velocity of 10^{-4} m/s was therefore applied to the wedge, which was assumed to be rigid.

The virtual crack closure method was used to calculate values of the strain-energy release-rate, G , as a crack was allowed to propagate through the specimen. This method, proposed by Rybicki & Kanninen [27] utilises the nodal forces at the crack tip and the nodal displacements at the next node (towards the crack mouth), see Fig. 17. The total strain-energy release-rate, G , is calculated from the relation:

$$G = \frac{1}{2\beta}(F_x\delta_x + F_y\delta_y) \quad (3)$$

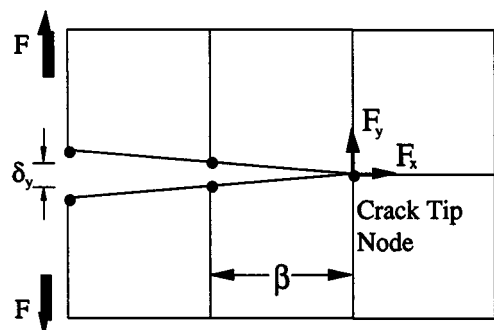


Figure 17 General finite-element mesh around crack tip, showing parameters for use with universal crack closure method to calculate the strain-energy release-rate, G , after [27].

where β is the crack-tip element width and F_x , F_y , δ_x and δ_y are the nodal forces and displacements in the x and y directions, respectively.

The load applied in the model was gradually increased and, as the applied strain-energy release-rate, G , at the crack tip reached the measured G_c value for the adhesive, the nodes along the centre of the adhesive layer were released in turn, as shown in Fig. 15. A time step was applied to the model, allowing the wedge to advance a fixed distance, and the value of G at the crack tip was then re-calculated. If the FE model could not reach a solution, or the value of G was higher than the measured value of G_c , the time step was reduced and the model run again using the same crack length. Similarly, if $G < G_c$, the time step was increased until the calculated value of the strain-energy release-rate, G , agreed with G_c to within an accuracy of $\pm 5\%$. Once the values of G and G_c agreed within this tolerance, a further set of nodes was released, and the process repeated. Approximately fifty increments of crack length were used between the point of initial contact of the wedge and the final failure of the specimen. A series of the FE predictions for the deformed shape of the IWP specimen during a typical modelling run is shown in Fig. 15.

7.2. Effect of friction

The contact between the wedge and the fractured surface of the adhesive was initially assumed to be frictionless. However, such a model predicted somewhat lower force values in the ‘plateau’ region of the IWP force versus time trace than those measured experimentally, see Table VI. Thus, friction between the wedge and the fractured surface of the adhesive of the specimen was included in the FE model. The literature [28] gives values of 0.4 to 0.5 for the coefficient of friction, μ , for the unlubricated contact between steel and a relatively hard, rigid polymer. Values of μ of both 0.4 and 0.5 give good agreement between the FE prediction and the experimental results, with the value of $\mu = 0.5$ giving the closest fit to the experimental data, as shown in Table VI.

As may be seen from Table VI, the use of a coefficient of friction lower than 0.5, for the same value of the adhesive fracture energy, gives somewhat lower values of the predicted cleavage force. However, the effect of friction is relatively small. Indeed, for the measured G_c

TABLE VI The effects of assumed values of G_c and coefficient of friction, μ , on the IWP cleavage force predicted by the finite-element modelling. (Steel substrates bonded with ‘XB5315’ adhesive, crack velocity of 10^{-4} m/s and test temperature of 23°C)

Coefficient of friction, μ	Adhesive fracture energy, G_c (kJ/m ²)	Predicted IWP cleavage force (N)
0	1.3	300
0	1.5	500
0.4	1.5	550
0.5	1.5	600

^aExperimental values of G_c and cleavage force were 1.5 kJ/m² and 600 N respectively.

of 1.5 kJ/m², a zero coefficient of friction gave a predicted cleavage force of 500 N, whilst a value of $\mu = 0.5$ gave a force of 600 N. By comparison, using a value of the adhesive fracture energy of 1.3 kJ/m², rather than the measured value of 1.5 kJ/m², gave a force of 300 N, as opposed to 500 N. (The experimentally measured value of the wedge cleavage force was 600 N.) Thus, neglecting friction has only a relatively small effect on the results from the FE model, compared with changing the value of the adhesive fracture energy, G_c . The predictions discussed below assume that the coefficient of friction between the wedge and the adhesive fracture surface is 0.5, and use the experimentally measured value of G_c of 1.5 kJ/m².

7.3. Comparison of modelling and experimental results

To predict the IWP cleavage force requires the material properties of the adhesive and substrates, i.e. the adhesive fracture energy of the adhesive, the stress versus strain data and the Poisson’s ratio, to be known. These data are given in Table IV and V. A coefficient of friction of 0.5 was assumed.

A series of the FE predictions of the deformed shape of the IWP specimen during a typical test is shown in Fig. 15. These results clearly show the extensive plastic deformation which accompanies the stable crack growth of the IWP test specimen. The agreement between the deformed shape of the specimen predicted by the FE model, and that observed experimentally, both visually and by using high-speed photography (see Fig. 7), is very good. Furthermore, the final, i.e. post-failure, predicted shape of the specimen corresponds very well to that observed experimentally. This may readily be seen if the final predicted image in Fig. 15 is compared with the photograph shown in Fig. 6a.

Examples of the predicted IWP force versus time response are shown in Fig. 18, for the steel and aluminium-alloy substrates bonded using the ‘XB5315’ adhesive. The assumption of purely elastic contact between the rigid wedge and the specimen probably leads to the predicted initial ‘peak’ response increasing somewhat more steeply than was seen experimentally. This is especially pronounced for the aluminium-alloy substrates. Nevertheless, the agreement between the finite-element predictions and the experimental results is extremely good. Indeed, the important values of the predicted IWP cleavage forces in the ‘plateau’ region are in excellent agreement with the experimentally recorded values.

The predicted IWP cleavage forces in the ‘plateau’ region for a range of adhesives used with both aluminium-alloy and steel substrates are shown in Table VII. The agreement between the predicted and the experimental values of the force is very good for the IWP tests undertaken with both the steel and aluminium-alloy substrates. It is noteworthy that the FE model also predicts a smaller IWP cleavage force for the aluminium-alloy substrates than for the steel substrates, for a given adhesive fracture energy, as indeed was observed experimentally.

TABLE VII Finite-element predictions of wedge-cleavage force from values of the adhesive fracture energy, G_c , together with experimentally-measured values. (Crack velocity of 10^{-4} m/s and test temperature of 23°C)

Adhesive	G_c , (kJ/m ²)	IWP cleavage force (N)			
		Aluminium-alloy substrates		Steel substrates	
		FE prediction	Experimental	FE prediction	Experimental
'AV119'	0.70	220	260	—	—
'XB5315'	1.55	450	350	600	600
'LMD1142'	4.59	—	—	1290	1580

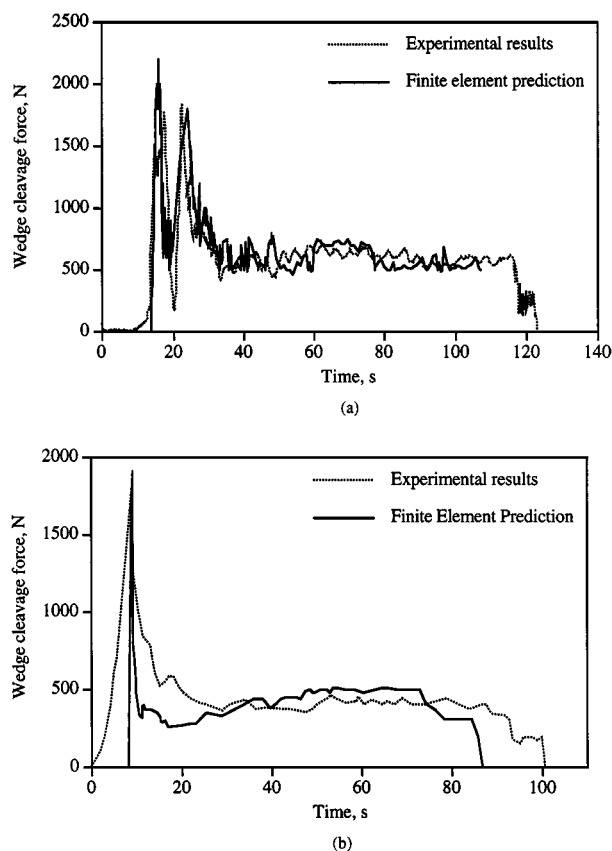


Figure 18 Finite-element predictions and experimental force versus time data for IWP specimens bonded with 'XB5315' adhesive. (a) steel substrates, (b) aluminium-alloy substrates.

8. Conclusions

The impact wedge-peel (IWP) test is an International Standard (ISO 11343) method that is employed to measure the resistance to cleavage fracture of structural adhesives. In the present work this test has been employed to evaluate the performance of a range of structural adhesives, when used to bond either steel or aluminium-alloy substrates. A novel test arrangement for performing these tests, using a high-speed servo-hydraulic machine, has been described. Tests were performed at rates of 10^{-4} and 2 m/s and at test temperatures of -40 and 23°C . High-speed photography was also used to investigate the failure of the IWP test specimens.

Firstly, both stable and unstable types of crack growth were recorded in the IWP test, with the crack propagating cohesively through the adhesive layer in all cases. The method of analysing the impact wedge-peel test results proposed by the ISO Standard has been found to give misleading results in some cases, for example when the specimen fails entirely by unstable crack prop-

agation. Hence, a preferred method of analysis has been identified and described. The use of this new method has shown that the impact wedge-peel test can provide good discrimination between adhesives possessing a range of toughnesses. However, the present work has shown that the measured IWP cleavage force depends on both the adhesive and the substrates used. Thus, like other types of peel test [29, 30], the IWP test has been found to reflect the fracture behaviour of the adhesive joint 'system', and not simply the adhesive in isolation. Thus, the mechanical properties of the substrates, which form the IWP joint, can greatly influence the results recorded from such tests.

Secondly, a linear correlation between the IWP cleavage-force and the adhesive fracture energy, G_c , measured using fracture-mechanics tests, has been identified. The gradient of this correlation is dependent on the properties of the substrate material used. However, the relationship between the IWP cleavage force and the adhesive fracture energy, G_c , does not appear to pass through the origin. Instead, a limiting value of G_c is observed, which represents a lower limit. Below this limiting value of G_c , the toughness of the adhesive is inadequate to enable sufficiently high stresses to be developed in the substrates to give rise to extensive plastic deformation of the arms of the substrate. Hence, unstable crack growth is seen in the IWP test specimen and a zero value of the wedge cleavage force is recorded. In contrast, for adhesives with G_c values above this limiting value, extensive plastic deformation of the arms of the substrates did occur, and stable crack propagation was observed in the IWP test. For such tests, relatively high values of the cleavage force were now recorded. This limiting value of G_c is dependent on the properties of the substrate material used.

Thirdly, the present work has described the development of a finite-element (FE) model to predict the IWP wedge-cleavage force versus time response, from knowledge of the value of G_c of the adhesive and the elastic-plastic properties of the substrate. The modelling work has shown that the effect of friction is relatively small, although the accuracy of the FE model was improved somewhat when friction between the wedge and the test specimen was included. The predicted values of the IWP wedge-cleavage force versus time response were in very good agreement with the values measured experimentally. The modelling work has also shown that a smaller cleavage force would be expected when aluminium-alloy substrates are used, compared with steel substrates, as was indeed seen experimentally. Further, the agreement between the deformed

shape of the IWP test specimen throughout the test, which is predicted by the FE model, is in excellent agreement with that observed experimentally.

Appendix—Specimen and forming specifications

Manufacture of preformed substrates: The substrates used for the Ford specimens were cut to size, and the loading hole was drilled through them. They were then pressed individually to preform them, using the loading hole to locate the substrate in the press, and the final dimensions used are shown in Fig. A1.

The substrates used for the Imperial College specimens were cut to size and clamped in a forming jig,

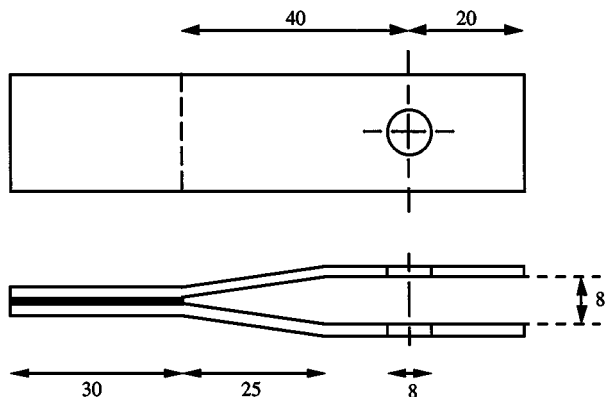


Figure A1 Ford specimen design. (All dimensions in millimetres.)

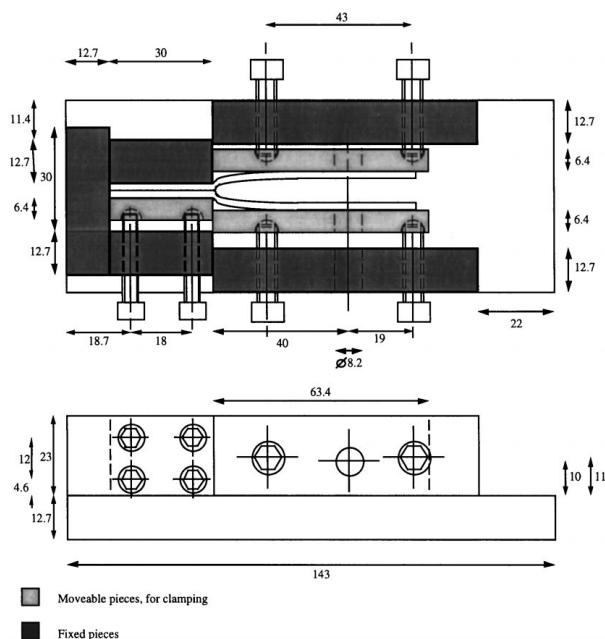


Figure A2 Forming jig used for Imperial College specimens. Dark shading on plan view indicates fixed pieces, and light shading indicates moveable pieces used for clamping. (All dimensions in millimetres.)

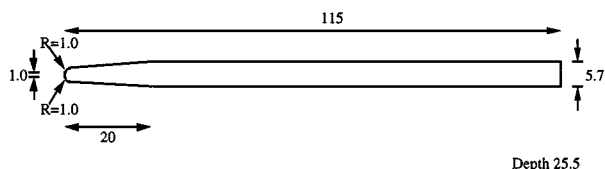


Figure A3 Forming wedge used for Imperial College specimens. (All dimensions in millimetres.)

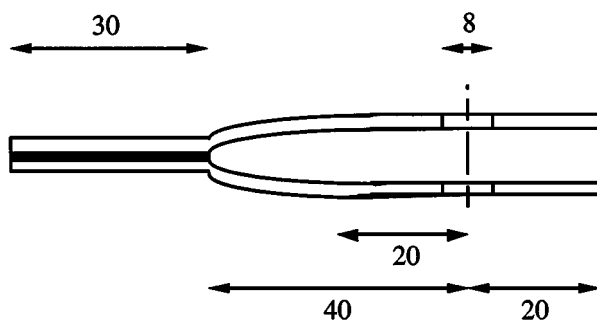


Figure A4 Imperial College specimen design. (All dimensions in millimetres.)

shown in Fig. A2. A forming wedge, shown in Fig. A3, was tapped between the free ends to preform the pair of substrates. A spacer was placed between the substrates, and the loading hole drilled. The final specimen dimensions are shown in Fig. A4.

Acknowledgements

The authors would like to thank the EPSRC, DTI MTS Programme and AEA Technology for their financial support. We would like to thank Roger Davis and Paul Fay at Ford Research and Brian Holmes at Ciba Polymers for their assistance. Thanks also to Tom Robinson, Hugh MacGillivray and Les Morris at Imperial College for their assistance with the manufacture of the test apparatus.

References

1. B. R. K. BLACKMAN, J. P. DEAR, A. J. KINLOCH, H. MACGILLIVRAY, Y. WANG, J. G. WILLIAMS and P. YAYLA, *J. Mater. Sci.* **30** (1995) 5885.
2. R. E. DAVIS and P. A. FAY, Ford Motor Company, Personal Communication (1993).
3. I. JANSSEN, Volvo Corporation, Personal Communication (1993).
4. P. A. FAY, R. E. DAVIS and G. D. SUTHURST, in Proceedings of Impact and Fatigue Testing of Adhesives, (Plastics & Rubber Institute, London, 1990).
5. R. A. DICKIE and S. M. WARD, in "Mittal Festschrift," edited by W. J. van Ooij and H. R. Anderson (VSP, Zeist, 1997) p. 1.
6. International Standards Organisation, ISO 11343 (ISO, Geneva, 1993).
7. B. HOLMES, Ciba Polymers, Personal Communication (1993).
8. European Structural Integrity Society (TC4), Plastics. Determination of fracture toughness (G_{Ic} and K_{Ic}) at high loading rates (ESIS, Delft, 1998) (Currently ISO CD 17281).
9. A. J. KINLOCH, G. K. A. KODOKIAN and F. JAMARANI, *J. Mater. Sci.* **22** (1987) 4111.
10. International Standards Organisation, ISO 291 (ISO, Geneva, 1997).
11. A. J. KINLOCH, "Adhesion and Adhesives: Science and Technology," (Chapman and Hall, London, 1987).
12. S. MOSTOVOY and E. J. RIPLING, *J. Applied Polymer Sci.* **10** (1966) 1351.
13. American Society for Testing and Materials, ASTM D3433-93 (ASTM, Philadelphia, 1993).
14. European Structural Integrity Society (TC4), Determination of the mode I adhesive fracture energy, G_{Ic} , of structural adhesives using the double cantilever beam and tapered double cantilever beam specimens (ESIS, Delft, 1997).
15. B. R. K. BLACKMAN, J. P. DEAR, A. J. KINLOCH, H. MACGILLIVRAY, Y. WANG, J. G. WILLIAMS and P. YAYLA, *J. Mater. Sci.* **31** (1996) 4451.

16. A. J. KINLOCH, B. R. K. BLACKMAN, A. C. TAYLOR and Y. WANG, in Proceedings of Euradh '96 (Institute of Materials, London, 1996) p. 467.
17. Y. WANG and J. G. WILLIAMS, *Int. J. Mech. Sci.* **38** (1996) 1073.
18. UK Defence Standard, 03-2/2 (1983).
19. S. MOSTOVOY, P. B. CROSLEY and E. J. RIPLING, *J. Materials* **2** (1967) 661.
20. A. J. KINLOCH and J. G. WILLIAMS, *J. Mater. Sci.* **15** (1980) 987.
21. A. C. TAYLOR, PhD thesis, Imperial College of Science, Technology and Medicine, University of London 1997.
22. P. L. TEED, "The Properties of Metallic Materials at Low Temperatures" (Chapman and Hall, London, 1950).
23. National Bureau of Standards, "Mechanical Properties of Metals and Alloys" (United States Department of Commerce, Washington, USA, 1943).
24. F. KING, "Aluminium and its Alloys" (Ellis Horwood, Chichester, 1987).
25. ASM International Handbook Committee, "Aluminium and Aluminium Alloys—ASM Specialty Handbook," edited by J. R. Davis, 2nd ed., (ASM, Washington, USA, 1994).
26. G. D. DEAN and B. C. DUNCAN, "Measurement, Technology and Standards Programme on the Performance of Adhesive Joints" (Department of Trade and Industry, London, 1994).
27. E. F. RYBICKI and M. F. KANNINEN, *Eng. Fracture Mech.* **9** (1977) 931.
28. A. GREER and D. J. HANCOCK, "Tables, Data and Formulae for Engineers" (Stanley Thornes, Cheltenham, 1984).
29. A. N. GENT and G. R. HAMED, *Polymer Eng. Sci.* **17** (1977) 462.
30. A. J. KINLOCH, C. C. LAU and J. G. WILLIAMS, *Int. J. Fracture* **66** (1994) 45.

*Received 10 June
and accepted 11 August 1999*